AD-A158 081 STEADY STATE PENETRATION OF RIGID PERFECTLY PLASTIC TARGETS(U) ARMY BALLISTIC RESEARCH LAB ABERDEEN PROVING GROUND MD R C BATRA ET AL. MAY 85 BRL-TR-2656 1/1

UNCLASSIFIED F/G 19/4 NL

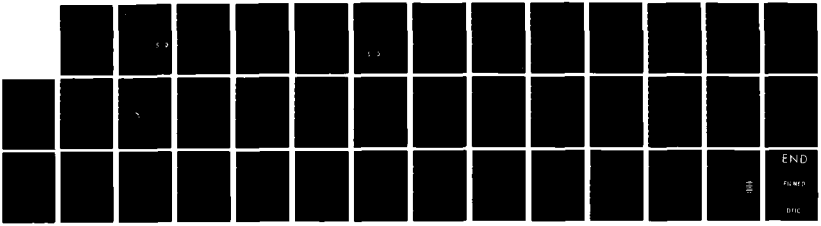

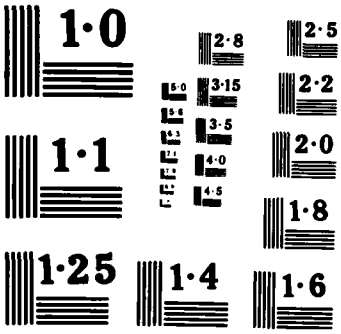

NATIONAL BUREAU OF STANDARDS
MICROCOPY RESOLUTION TEST CHART

AD-A158 081

(2)

AD

US ARMY
MATERIEL
COMMAND

TECHNICAL REPORT BRL-TR-2656

STEADY STATE PENETRATION OF RIGID PERFECTLY PLASTIC TARGETS

Romesh C. Batra
Thomas W. Wright

May 1985

DTIC
ELECTE
JUL 29 1985
S D
B

DTIC FILE COPY

APPROVED FOR PUBLIC RELEASE; DISTRIBUTION UNLIMITED.

US ARMY BALLISTIC RESEARCH LABORATORY
ABERDEEN PROVING GROUND, MARYLAND

85 7 29 017

Destroy this report when it is no longer needed.
Do not return it to the originator.

Additional copies of this report may be obtained from the National Technical Information Service, U. S. Department of Commerce, Springfield, Virginia 22161.

The findings in this report are not to be construed as an official Department of the Army position, unless so designated by other authorized documents.

The use of trade names or manufacturers' names in this report does not constitute indorsement of any commercial product.

UNCLASSIFIED

SECURITY CLASSIFICATION OF THIS PAGE (When Data Entered)

REPORT DOCUMENTATION PAGE

READ INSTRUCTIONS BEFORE COMPLETING FORM

1. REPORT NUMBER
TECHNICAL REPORT BRL-TR-2656

2. GOVT ACCESSION NO.
AD-A158 081

3. RECIPIENT'S CATALOG NUMBER

4. TITLE (and Subtitle)
Steady State Penetration of Rigid Perfectly Plastic Targets

5. TYPE OF REPORT & PERIOD COVERED

6. PERFORMING ORG. REPORT NUMBER

7. AUTHOR(s)
Romesh C. Batra* and Thomas W. Wright

8. CONTRACT OR GRANT NUMBER(s)

9. PERFORMING ORGANIZATION NAME AND ADDRESS
US Army Ballistic Research Laboratory
ATTN: AMXBR-TBD
Aberdeen Proving Ground, MD 21005-5066

10. PROGRAM ELEMENT, PROJECT, TASK AREA & WORK UNIT NUMBERS

11. CONTROLLING OFFICE NAME AND ADDRESS
US Army Ballistic Research Laboratory
ATTN: AMXBR-OD-ST
Aberdeen Proving Ground, MD 21005-5066

12. REPORT DATE
May 1985

13. NUMBER OF PAGES
38

14. MONITORING AGENCY NAME & ADDRESS (if different from Controlling Office)

15. SECURITY CLASS. (of this report)
UNCLASSIFIED

15a. DECLASSIFICATION/DOWNGRADING SCHEDULE

16. DISTRIBUTION STATEMENT (of this Report)
Approved for public release; distribution unlimited.

17. DISTRIBUTION STATEMENT (of the abstract entered in Block 20, if different from Report)

18. SUPPLEMENTARY NOTES
*University of Missouri - Rolla
Department of Engineering Mechanics
Rolla, MO 65401-0249

19. KEY WORDS (Continue on reverse side if necessary and identify by block number)

20. ABSTRACT (Continue on reverse side if necessary and identify by block number)
The problem of steady penetration by a semi-infinite, rigid penetrator into an infinite, rigid/perfectly plastic target has been studied. The rod is assumed to be cylindrical, with a hemispherical nose, and the target is assumed to obey the Von Mises yield criterion with the associated flow rule. Contact between target and penetrator has been assumed to be smooth and frictionless. Results computed and presented graphically include the velocity field in the target, the tangential velocity of target particles on the penetrator nose, normal pressure over the penetrator nose, and the dependence of the axial resisting

DD FORM 1 JAN 73 1473 EDITION OF 1 NOV 65 IS OBSOLETE

UNCLASSIFIED

SECURITY CLASSIFICATION OF THIS PAGE (When Data Entered)

force on penetrator speed and target strength.

TABLE OF CONTENTS

		Page
	LIST OF ILLUSTRATIONS	5
I.	INTRODUCTION	7
II.	FORMULATION OF THE PROBLEM	8
III.	FINITE ELEMENT FORMULATION OF THE PROBLEM	10
IV.	COMPUTATION AND DISCUSSION OF RESULTS	13
V.	CONCLUSIONS	27
	REFERENCES	29
	DISTRIBUTION LIST	31

DTIC
ELECTE
JUL 29 1985
S D
B

Accession For
NTIS GRA&I
DTIC TAB
Unannounced
Justification
By
Distribution/
Availability Codes
Dist | Avail and/or Special
A-1

LIST OF ILLUSTRATIONS

FIG. NO.		Page
1	The Region to be Studied.	11
2	Finite Element Grid Used.	14
3	Velocity Field in the Target Material (α = 4.0).	15
4	Normal Stress Distribution on the Hemispherical Nose of the Penetrator	16
5	Axial Force vs. α.	18
6	Contours of p in the Target	19
7	Variation of $-\sigma_{zz}$ at Points of the Target Along the Axis Ahead of the Penetrator	20
8	Tangential Velocity Distribution on the Hemispherical Nose of the Penetrator.	21
9	Variation of the z-Velocity of Target Particles Along the Axis Ahead of the Penetrator.	22
10	Variation of v_z With r on the Surface z = 0	24
11	Variation of v_z With r on the Surface z = - 1.595.	25
12	Comparison of Stresses Calculated in this Paper and in Pidsley[7].	26
13	Contributions to the Integral Formula (12).	28

PREVIOUS PAGE IS BLANK

I. INTRODUCTION

In simple theories of penetration the material properties of target and penetrator are often represented only by constant characteristic stresses, as for example in Tate.[1,2] Although this approach leads to results that are qualitatively correct, it can be difficult to use quantitatively. Some of the problems have to do with actual deformations in target and penetrator including lateral motion, and others are associated with the fact that the plastic flow stress is determined only by the deviatoric components of stress whereas the spherical or pressure component, which may be quite large ahead of the penetrator and contributes significantly to the retardation of the penetrator, is unrelated to flow stress. These and other matters have been discussed recently in some detail by Wright.[3] It would be desirable to account for lateral motion and hydrostatic effects in some simple way, but at present the details are insufficiently known to suggest high quality approximations that might be suitable. In developing an engineering model for penetration and perforation, Ravid and Bodner[4] have attempted to meet this difficulty be assuming simple kinematics for the flow around the penetrator and then adjusting some unknown parameters so as to minimize the plastic dissipation. They characterize this procedure as being "a modification of the upper bound theorem of plasticity to include dynamic effects," but even if such a modified theorem is actually valid, at present there is no way to tell how close such a bound might be.

In this paper a detailed numerical solution to an idealized penetration problem is presented in an attempt to shed some light on these matters. The approach taken is as follows. Suppose that the penetrator is in the intermediate stages of penetration so that the active target/penetrator interface is at least one or two penetrator diameters away from either target face, and the remaining penetrator is still much longer than several diameters and is still traveling at a speed close to its striking velocity.

This situation is idealized here in several ways. First, it is assumed that the rod is semi-infinite in length and that the target is infinite with a semi-infinite hole. Furthermore, it is assumed that the rate of penetration and all flow fields are steady as seen from the nose of the penetrator. These approximations are reasonable if the major features

---

[1] *Tate, A., "A Theory for the Deceleration of Long Rods After Impact," J. Mech. Phys. Sol. 15, 1967, 387-399.*

[2] *Tate, A., "Further Results in the Theory of Long Rod Penetration," J. Mech. Phys. Sol. 17, 1969, 141-150.*

[3] *Wright, T.W., "A Survey of Penetration Mechanics for Long Rods," in Lecture Notes in Engineering, Vol. 3, Computational Aspects of Penetration Mechanics, Eds., J. Chandra and J. Flaherty, Springer-Verlag, New York, 1983.*

[4] *Ravid, M. and Bodner, S.R., "Dynamic Perforation of Visco-plastic Plates by Rigid Projectiles," Int. J. Eng. Sci. 21, 1983, 577-591.*

PREVIOUS PAGE IS BLANK

of the plastic flow field become constant within a diameter or so of the nose of the penetrator, and will be justified a posteriori by the calculation.

Next, it is assumed that no shear stress can be transmitted across the target/penetrator interface. This is justified on the grounds that a thin layer of material at the interface either melts or is severely degraded by adiabatic shear. This assumption, together with the previous one, makes it possible to decompose the problem into two parts in which either a rigid rod penetrates a deformable target or a deformable rod is upset at the bottom of a hole in a rigid target. Of course, in the combined case the contour of the hole is unknown, but if it can be chosen so that normal stresses match in the two cases along the whole boundary between penetrator and target, then the complete solution is known irrespective of the relative motion at the boundary. Even without matching the normal stresses, it would seem that valuable qualitative information about the flow field and distribution of stresses can be gained if the chosen contour is reasonably close to those that are actually observed in experiments.

Finally, the deforming material is assumed to be rigid/perfectly plastic. This assumption should be adequate for examining the flow and stress fields near the penetrator nose, but will lose accuracy with increasing distance, since it forces the effects of compressibility and wave propagation to be ignored.

In this paper only the case of the deforming target and a rigid penetrator is considered, where the penetrator is assumed to have a circular cylindrical body and a hemispherical nose.

II. FORMULATION OF THE PROBLEM

With respect to a set of cylindrical coordinate axes fixed to the center of the hemispherical nose of the rigid cylindrical penetrator, equations governing the deformations of the target are

$$\begin{aligned} \operatorname{div}\underset{\sim}{v} &= 0, \\ \operatorname{div}\underset{\sim}{\sigma} &= \rho\dot{\underset{\sim}{v}} = \rho(\underset{\sim}{v}\cdot\operatorname{grad})\underset{\sim}{v}. \end{aligned} \tag{1}$$

Here $\underset{\sim}{\sigma}$ is the Cauchy stress tensor, ρ is the mass density of the target material, $\underset{\sim}{v}$ is the velocity of a target particle relative to the penetrator, which has absolute velocity $v_o\,\underset{\sim}{e}$, $\underset{\sim}{e}$ being a unit vector along the axis and in the direction of motion of the penetrator. The operators grad and div signify the gradient and divergence operators on fields defined in the present configuration. Equation $(1)_1$ expresses the balance of mass and implies that the target undergoes only volume preserving deformations so that the mass density of the target stays constant. Equation $(1)_2$ expresses the balance of linear momentum in the absence of body forces and holds in all Galilean coordinate systems. In particular it holds in one that translates at the constant velocity of the penetrator. Equation $(1)_3$

holds only in such a translating system where all field variables are independent of time. The target material is assumed to obey the Von-Mises yield criterion and the associated flow rule. That is (Prager and Hodge),[5]

$$\underset{\sim}{\sigma} = -p\underset{\sim}{1} + \frac{\sigma_o}{\sqrt{3I}}\underset{\sim}{D} ,$$

$$\underset{\sim}{D} = (\text{grad}\underset{\sim}{v} + (\text{grad}\underset{\sim}{v})^T)/2 \qquad (2)$$

$$I = \frac{1}{2}\,\text{tr}\,(\underset{\sim}{D}^2).$$

In equations (2) p is the hydrostatic pressure (which, of course, cannot be determined by the deformation because of the assumption of incompressibility), $\underset{\sim}{1}$ is the identity matrix, $\underset{\sim}{D}$ is the strain rate tensor, σ_o is the flow stress of the target material in simple compression and $\text{tr}(\underset{\sim}{D}_2)$ equals the sum of the diagonal terms of the square matrix $\underset{\sim}{D}$. Equation $(2)_1$ is the constitutive relation of an incompressible Navier-Stokes fluid with viscosity coefficient equal to $\sigma_o/2\sqrt{3I}$. Equations (2), when substituted into $(1)_3$, give the field equation

$$-\text{grad}\,p + \sigma_o\text{div}((\text{grad}\underset{\sim}{v} + (\text{grad}\underset{\sim}{v})^T)/2\sqrt{3I}) = \rho(\underset{\sim}{v}\cdot\text{grad})\underset{\sim}{v} \qquad (3)$$

which together with $(1)_1$ is to be solved for p and $\underset{\sim}{v}$ subject to suitable boundary conditions. Before stating these the following non-dimensional variables will be introduced.

$$\bar{\underset{\sim}{\sigma}} = \underset{\sim}{\sigma}/\sigma_o, \quad \bar{\underset{\sim}{v}} = \underset{\sim}{v}/v_o, \quad \bar{r} = r/r_o, \quad \bar{z} = z/r_o, \quad \bar{p} = p/\sigma_o .$$

The pair (r,z) denotes the cylindrical coordinates of a point with respect to axes attached to the center of the hemispherical nose with the positive z-axis pointing into the target material. Rewriting equations $(1)_1$ and (3) in terms of non-dimensional variables, dropping the superimposed bars, and agreeing to denote the gradient and divergence operators in non-dimensional coordinates by grad and div, we arrive at the following set of equations.

$$\begin{aligned} &\text{div}\underset{\sim}{v} = 0 \\ &-\text{grad}\,p + \text{div}\,((\text{grad}\underset{\sim}{v} + (\text{grad}\underset{\sim}{v})^T)/2\sqrt{3I}) = \alpha(\underset{\sim}{v}\,\text{grad})\underset{\sim}{v}, \end{aligned} \qquad (4)$$

where $\alpha = \rho v^2/\sigma o$ is a non-dimensional number.

---

[5] *Prager, W. and Hodge, P., Theory of Perfectly Plastic Solids, Dover Publ., New York, 1968.*

Boundary conditions must be given both for the penetrator/target interface and for points remote from the penetrator. As stated in the introduction the interface conditions are

$$\begin{aligned} \underset{\sim}{t} \cdot (\underset{\sim}{\sigma}\underset{\sim}{n}) &= 0, \\ \underset{\sim}{v} \cdot \underset{\sim}{n} &= 0, \end{aligned} \tag{5}$$

where $\underset{\sim}{n}$ is a unit normal on the surface and $\underset{\sim}{t}$ is a unit tangent on the surface. At points far away from the penetrator,

$$\begin{aligned} &|\underset{\sim}{v} + v_o\underset{\sim}{e}| \to 0 \quad \text{as } |\underset{\sim}{x}| = (r^2 + z^2)^{1/2} \to \infty, \; z > -\infty, \\ &|\underset{\sim}{\sigma}\underset{\sim}{n}| \to 0 \quad \text{as } z \to -\infty, \end{aligned} \tag{6}$$

where $\underset{\sim}{e}$ is a unit vector in the positive z-direction, as before. The boundary conditions (5) state that the contact surfaces between target and penetrator are smooth and there is no interpenetration of the target material into the penetrator or vice versa. The boundary condition $(6)_1$ is equivalent to the statement that target particles at a large distance from the penetrator appear to be moving at a uniform speed with respect to it. Equation $(6)_2$ states that far to the rear the traction field vanishes. Note that the governing equations (3) are nonlinear in $\underset{\sim}{v}$ and that a solution of $(1)_1$ and (3) under the stated boundary conditions, if there is one, will depend on the rates at which the quantities in (6) tend towards zero.

III. FINITE ELEMENT FORMULATION OF THE PROBLEM

In order to solve the problem numerically, it is possible to consider only a finite region of the target, and since deformations of the target are axisymmetric, only the target region shown in Figure 1 is studied. Whether the region considered is adequate or not can be easily decided by solving the problem for two different values of the parameter a. If the two solutions so obtained are essentially equal to each other in the vicinity of the penetrator, then the region studied is sufficient and the effect of boundary conditions at the outer surface EFA has a negligible effect on the deformations of the target material in close proximity to the penetrator. The boundary conditions imposed on the finite region are

$$\begin{aligned} &\sigma_{zz} = 0, \quad v_r = 0 \quad \text{on the bottom surface AB}, \\ &\underset{\sim}{t} \cdot \underset{\sim}{\sigma}\underset{\sim}{n} = 0, \quad \underset{\sim}{v} \cdot \underset{\sim}{n} = 0 \quad \text{on the common interface BCD}, \\ &\sigma_{rz} = 0, \quad v_r = 0 \quad \text{on the axis of symmetry DE}, \\ &v_r = 0, \quad v_z = -1.0 \quad \text{on the bounding surface EFA}. \end{aligned} \tag{7}$$

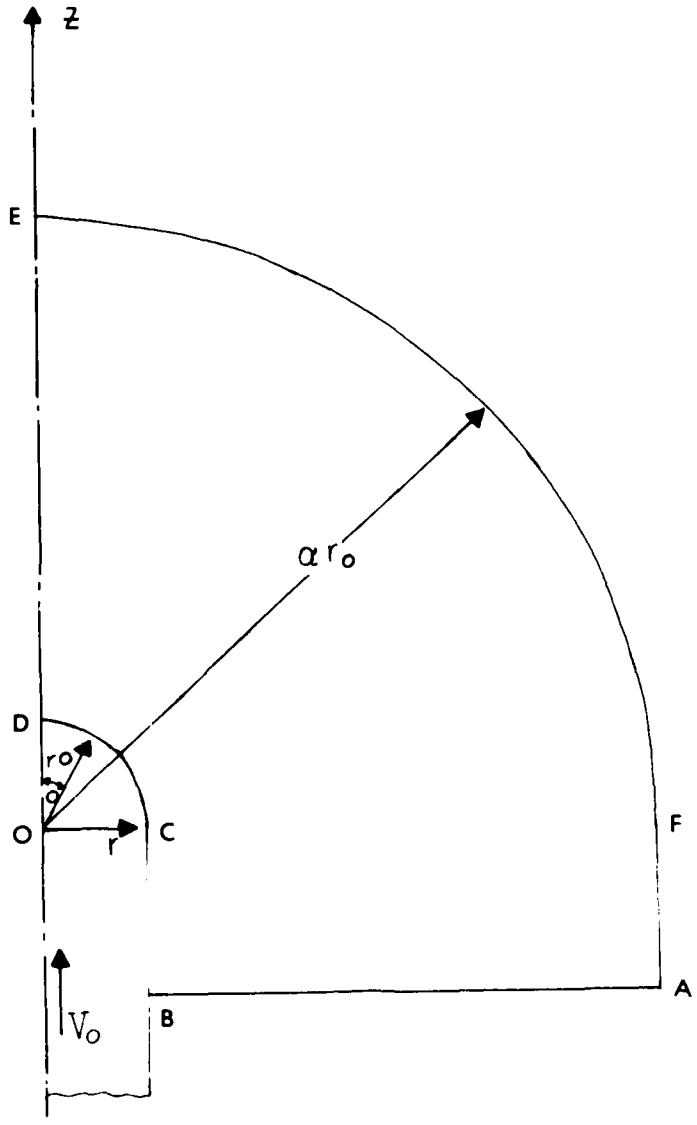

Figure 1: The Region to be Studied.

A weak formulation of the problem is now obtained. Let $\underset{\sim}{\phi}$ be a smooth, vector valued function defined on the region R of the target shown in Figure 1, where $\underset{\sim}{\phi}$ satisfies the velocity boundary conditions included in equations $(7)_1$ - $(7)_3$ and $\underset{\sim}{\phi} = 0$ on the surface EFA. In addition let ψ be a bounded, scalar valued function defined on R. Taking the inner product of both sides of equation $(4)_1$ with $\underset{\sim}{\phi}$ and of equation $(4)_2$ with $\underset{\sim}{\phi}$, integrating the resulting equations over R, using the divergence theorem, the stress boundary conditions in (7) and the stated boundary conditions for $\underset{\sim}{\phi}$, we arrive at the following equations.

$$\int_R \psi(\mathrm{div}\underset{\sim}{v})\ dV = 0\ ,$$

$$-\int_R p(\mathrm{div}\underset{\sim}{\phi})\ dV + \int_R \frac{1}{2\sqrt{3I}}\ \underset{\sim}{D}:(\mathrm{grad}\underset{\sim}{\phi} + (\mathrm{grad}\underset{\sim}{\phi})^T)\ dV \tag{8}$$

$$= \alpha\int_R (\underset{\sim}{v}\cdot\mathrm{grad})\underset{\sim}{v}\ \cdot\ \underset{\sim}{\phi}\ dV.$$

The boundary value problem defined by equations (4) and (7) is equivalent to the statement that equations (8) hold for every $\underset{\sim}{\phi}$ and ψ such that grad $\underset{\sim}{\phi}$ and ψ are square integrable over R, $\underset{\sim}{\phi}$ satisfies the stated homogeneous boundary conditions, and $\underset{\sim}{v}$ satisfies all the velocity boundary conditions stated in (7).

An approximate solution of equations (8) has been obtained by using the finite element method (see Becker, Carey, and Oden[6] for details). Since equation $(8)_2$ is nonlinear in $\underset{\sim}{v}$, the following iterative technique has been used.

$$\int_R \psi(\mathrm{div}\underset{\sim}{v}^m)\ dV = 0$$

$$-\int_R p^m(\mathrm{div}\underset{\sim}{\phi})\ dV + \int_R \frac{1}{2\sqrt{3I^{m-1}}}\ \underset{\sim}{D}^m:(\mathrm{grad}\underset{\sim}{\phi} + (\mathrm{grad}\underset{\sim}{\phi})^T)\ dV \tag{9}$$

$$= \alpha\int_R (\underset{\sim}{v}^{m-1}\cdot\ \mathrm{grad})\underset{\sim}{v}^m\ \cdot\ \underset{\sim}{\phi}\ dV,$$

---

[6] Becker, E., Carey, G., and Oden, J.T., *Finite Elements, An Introduction*, Vol. 1, Prentice-Hall, Englewood Cliffs, NJ, 1981.

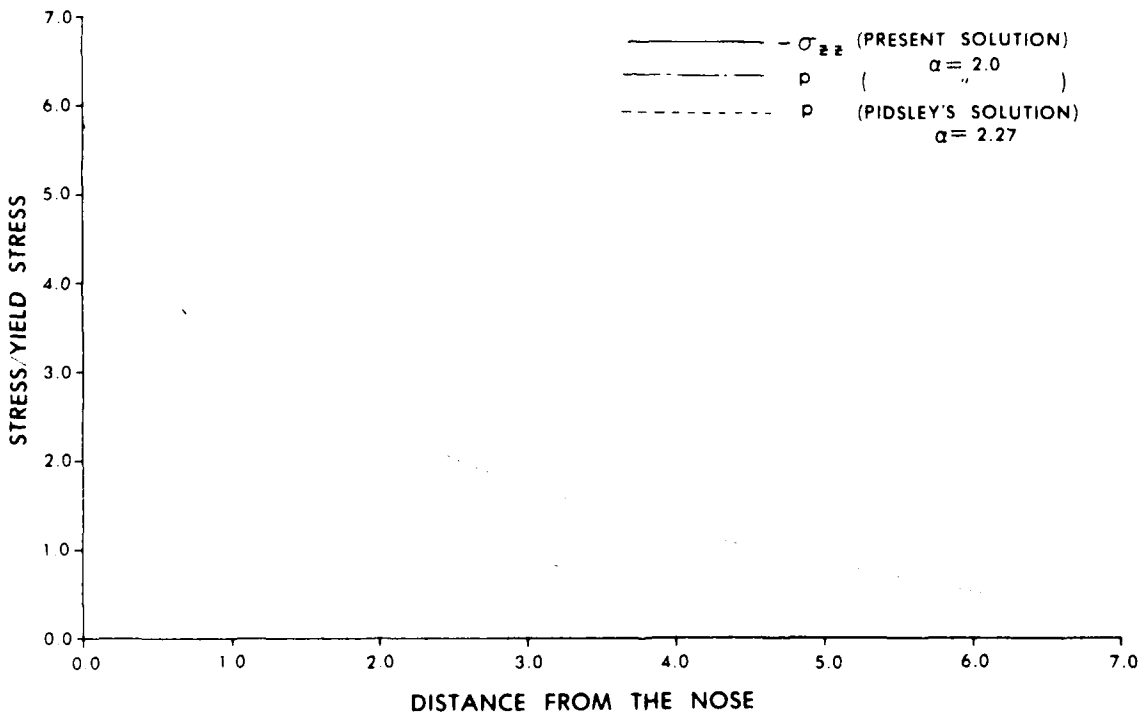

Figure 12: Comparison of Stresses Calculated in this Paper and in Pidsley[7].

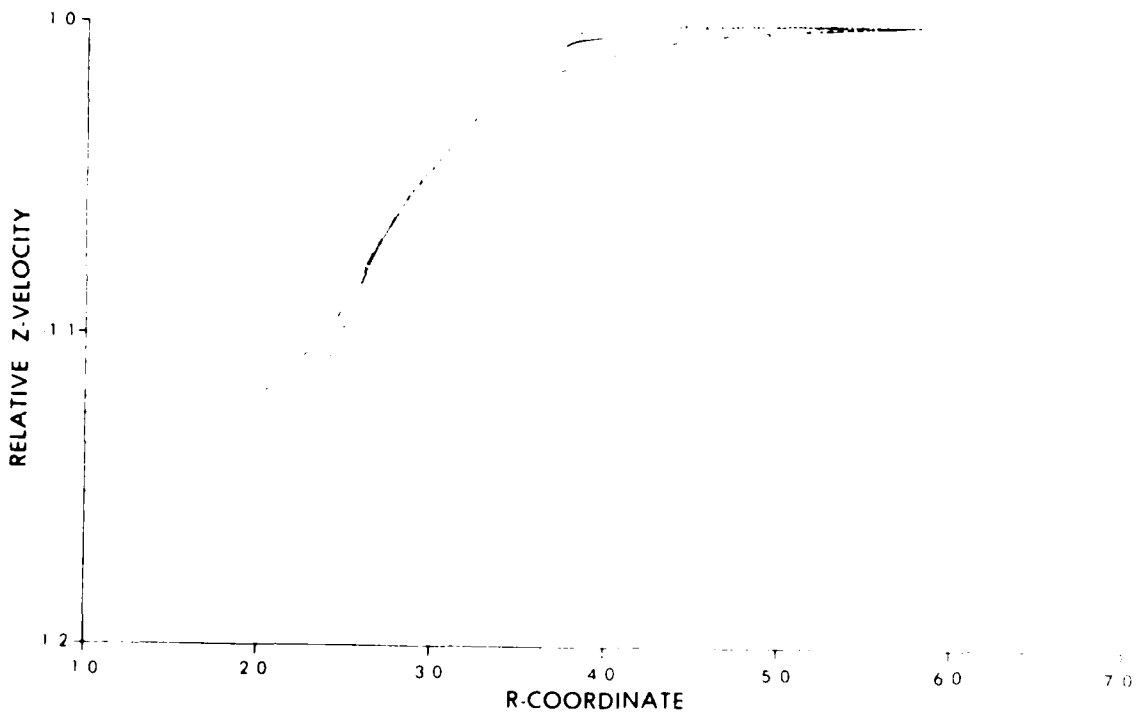

Figure 11: Variation of v_z With r on the Surface z = - 1.595.

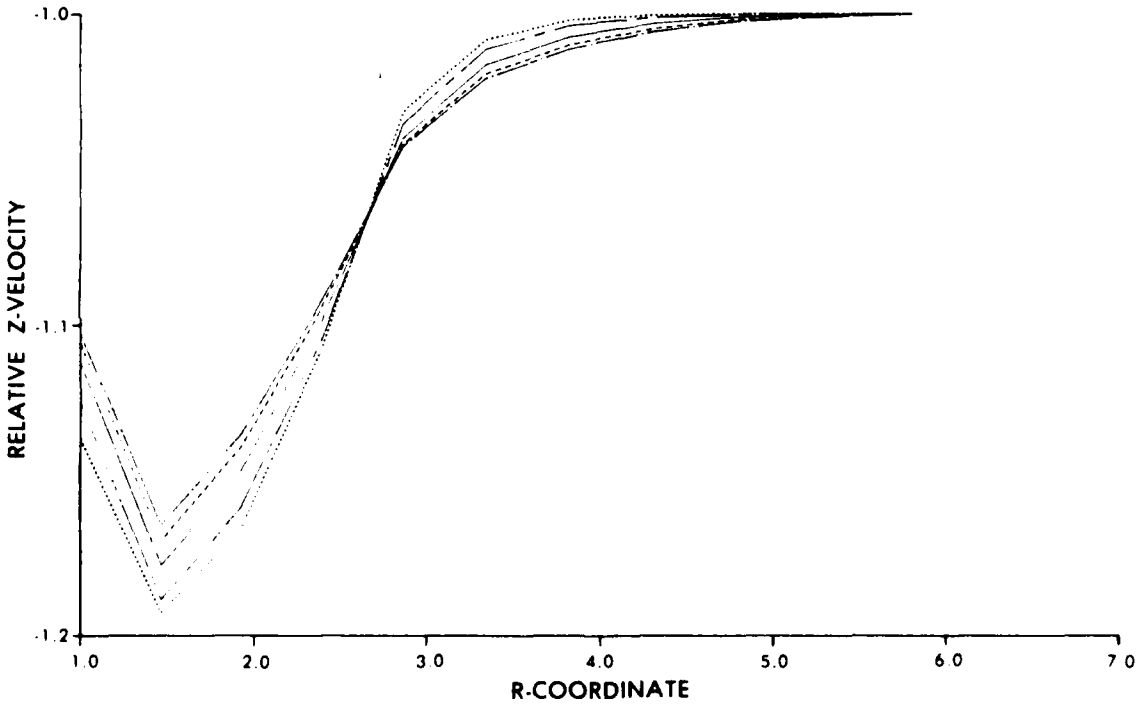

Figure 10: Variation of v_z With r on the Surface z = 0.

deformation extends only to about one or two radii away from the nose, whereas the stress is still significant at three radii. The nondimensional values of $\sqrt{I}$, computed for $\alpha = 6.15$, become as large as 2.0 or 2.5 at points close to the nose tip. Since true strain rates scale with v_o/r_o, actual rates in the target may easily be of the order of $10^5 s^{-1}$ or more for reasonable values of v_o and r_o. Thus, strain rate effects may become important in some cases. This should be borne in mind especially for small scale experimental studies, which will accentuate rate effects and tend to make target materials appear stronger in small scale than in full scale.

Figures 10 and 11 show the variation of v_z with r at z = 0 and z = -1.595, respectively. These results indicate that more of the target material at the sides of the penetrator deforms at higher values of α, even though this is not true ahead of the penetrator as noted in the discussion of Figure 9. In both Figure 10 and 11 the nondimensional velocity near the penetrator decreases in absolute value with increasing α in order to satisfy the balance of mass. That is to say, since the deformations of the target are volume preserving, the areas between each curve and $v_z = -1.0$ must be constant and just large enough to account for the rate of increase of hole volume as the penetrator advances into the target. Thus the effect of inertia is to spread the deformation farther to the sides, for which compensation must be made closer in so as to maintain incompressibility.

In a recent paper, Pidsley[7] described an unsteady calculation for one impact velocity in which both target and penetrator were assumed to be compressible and elastic/perfectly plastic. He shows that after a few diameters penetration, the rate of penetration slows down and approaches a steady state. Figure 12 compares his values of pressure with the present values of pressure and axial stress along the centerline ahead of the penetrator for nearly the same values of α. Compressibility apparently has the effect of reducing the pressure directly in front of the penetrator and increasing it at distances greater than one penetrator radius or so, but even so, the results seem to be broadly similar. It has not been possible to compare velocity fields. In his paper Pidsley[7] also notes that if the equation of motion for steady flow is integrated along the central streamline, there is a contribution from transverse gradients of shear stress, unlike the case for a perfect fluid. This fact, which was also noted by Wright,[3] may be expressed in the following formula.

$$\frac{1}{2}\rho v^2 + p - s_{zz} - 2\int_0^z \frac{\partial \sigma_{rz}}{\partial r}\, dz = -\sigma_{zz}(0) \qquad (12)$$

---

[7] Pidsley, P. H., *"A Numerical Study of Long Rod Impact Onto a Large Target," J. Mech. Phys. Sol. 32, 1984, 315-333.*

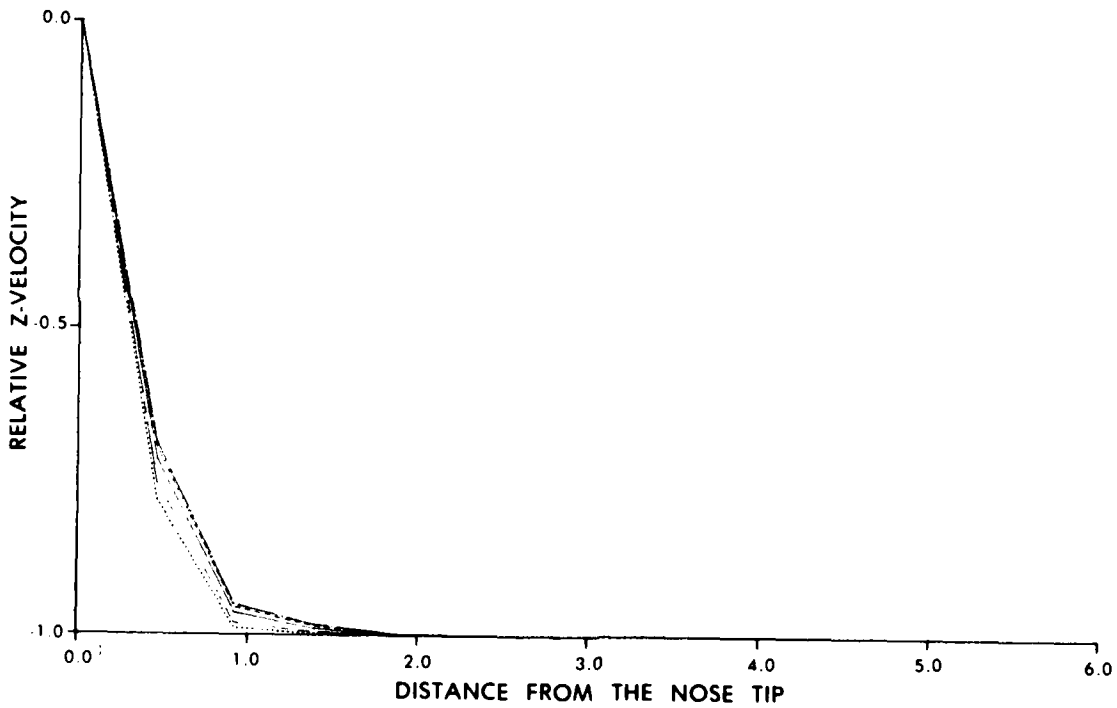

Figure 9: Variation of the z-Velocity of Target Particles Along the Axis Ahead of the Penetrator.

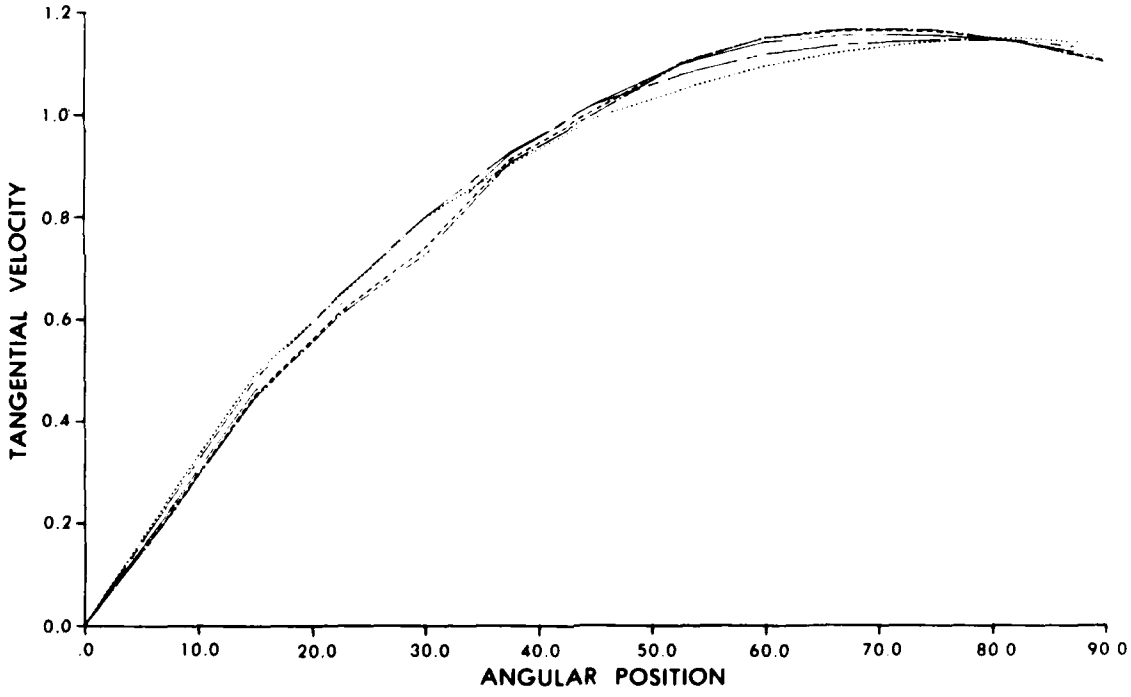

Figure 8: Tangential Velocity Distribution on the Hemispherical Nose of the Penetrator.

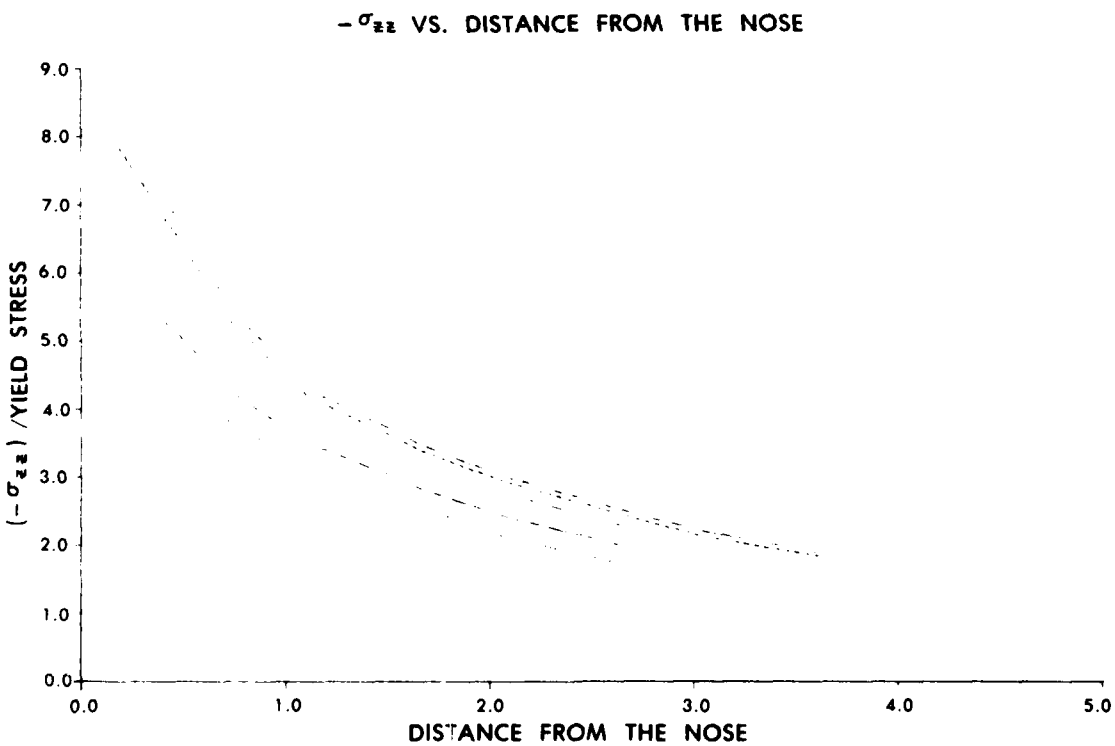

Figure 7: Variation of $-\sigma_{zz}$ at Points of the Target Along the Axis Ahead of the Penetrator.

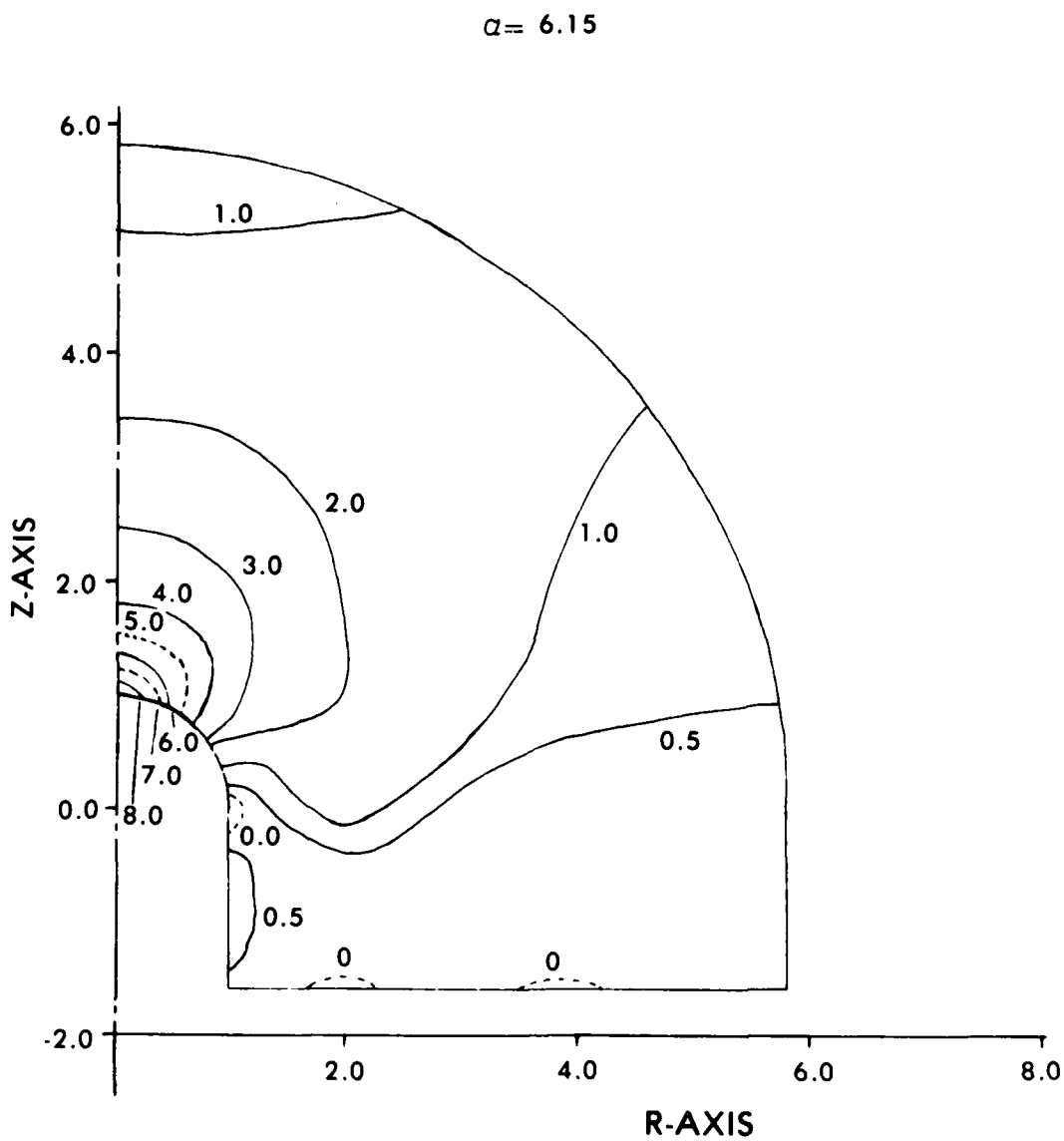

Figure 6: Contours of p in the Target.

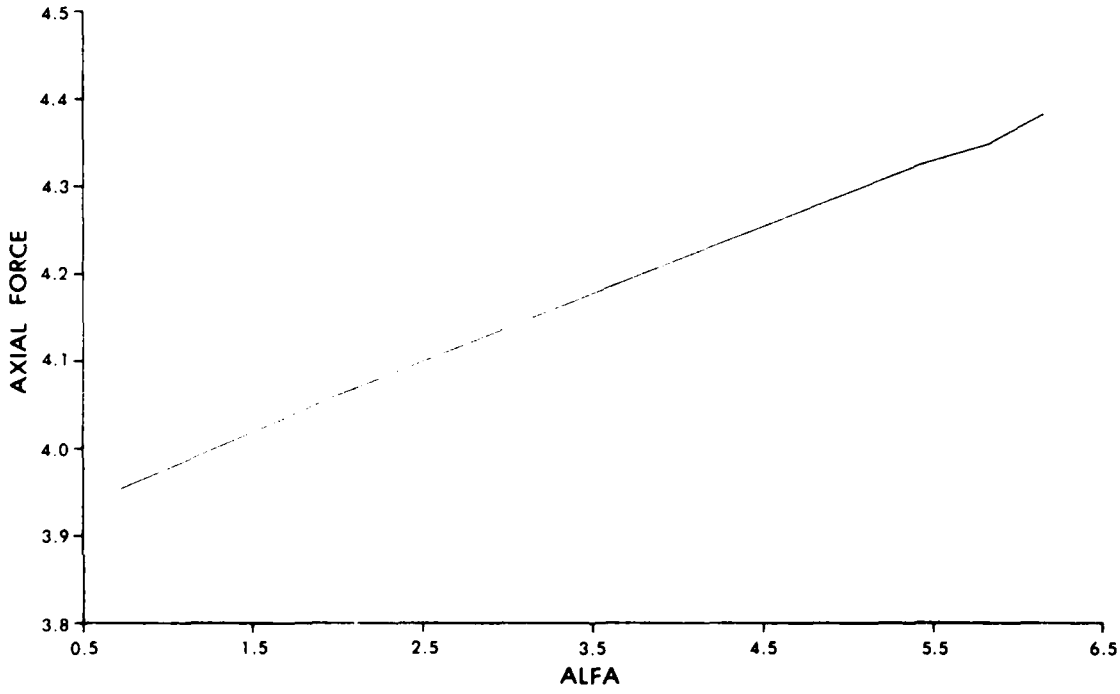

Figure 5: Axial Force vs. α.

Table 1. Legend for Figures

Curve Type	α
. . . . .	0.72
----- - ----- -	2.00
----------	4.00
- - - - - - - -	5.43
_____ . _____ .	6.15

The total nondimensional force (average stress/flow stress) that acts on the penetrator nose in the negative axial direction is given by

$$F = \int_0^{\pi/2} (\underset{\sim}{n} \cdot \underset{\sim}{\sigma}\underset{\sim}{n}) \sin 2\theta \, d\theta .$$

Figure 5, which is a plot of F versus α, shows that F increases only weakly and nearly linearly with α. A close approximation to the line is given by the equation

$$F = 3.903 + 0.0773\alpha , \tag{11}$$

so that in typical impact problems, where the rate of penetration lies roughly in the range $2 \leq \alpha \leq 6$, the retarding force varies only from about 4.1 to 4.4 times the product of cavity area and compressive flow stress in the target material. Of course this range may change with nose shape, but it does seem to indicate why the choice of constant target resistance in the simple theory of Tate[1,2] gives such good qualitative results. Note also, that for the same range of α, the centerline stress on the penetrator nose, as shown in Figure 4, varies from about 5.3 to 8.8 or as much as twice the average value.

That a significant contribution to the axial force is made by the spherical component of the Cauchy stress $\underset{\sim}{\sigma}$ is clear from Figure 6, which shows values of non-dimensional p in the target. Whereas the deviatoric components of $\underset{\sim}{\sigma}$ have magnitudes comparable to the flow stress σ_o, the spherical component p is more than 8 times σ_o near the nose tip. Figure 7 shows the principal stress component $-\sigma_{zz}$ along the axis in front of the penetrator and demonstrates that stress falls rapidly with distance. The stress near three radii for the smaller values of α cannot be accurately calculated since the velocity gradient there is extremely small.

Figure 8 shows that the nondimensional velocity of target particles, tangential to the penetrator nose, is essentially independent of α, and Figure 9 shows that the same is true for the axial velocity of target particles along r = 0 ahead of the penetrator. Note that the velocity falls more rapidly than stress ahead of the penetrator so that target

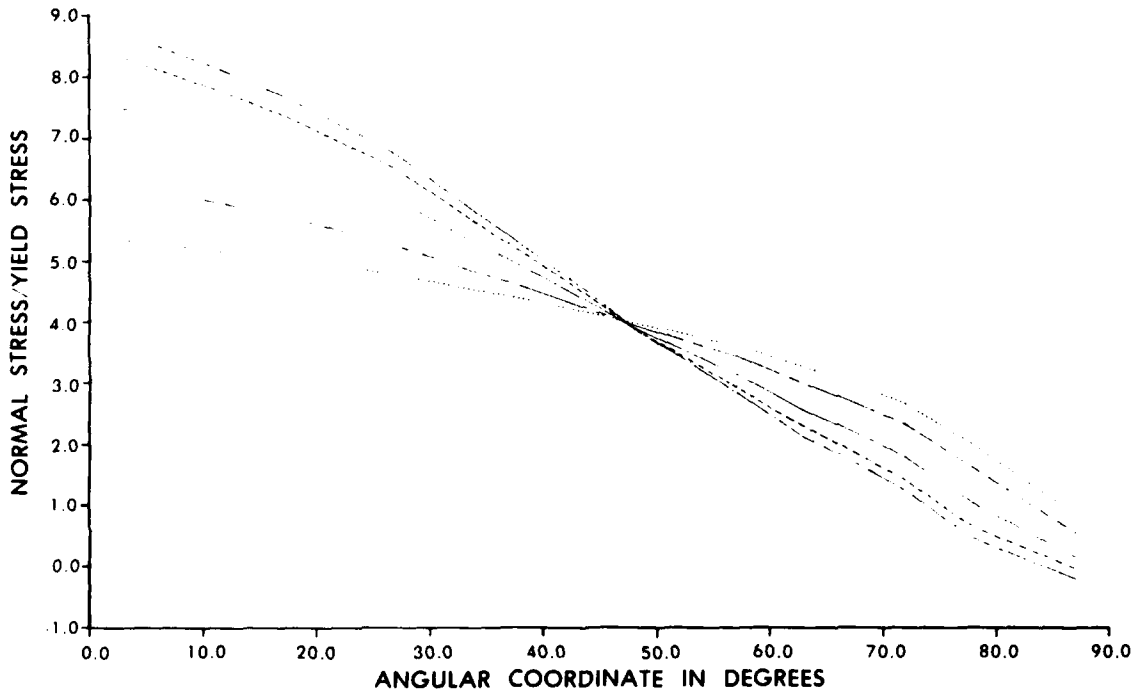

Figure 4: Normal Stress Distribution on the Hemispherical Nose of the Penetrator.

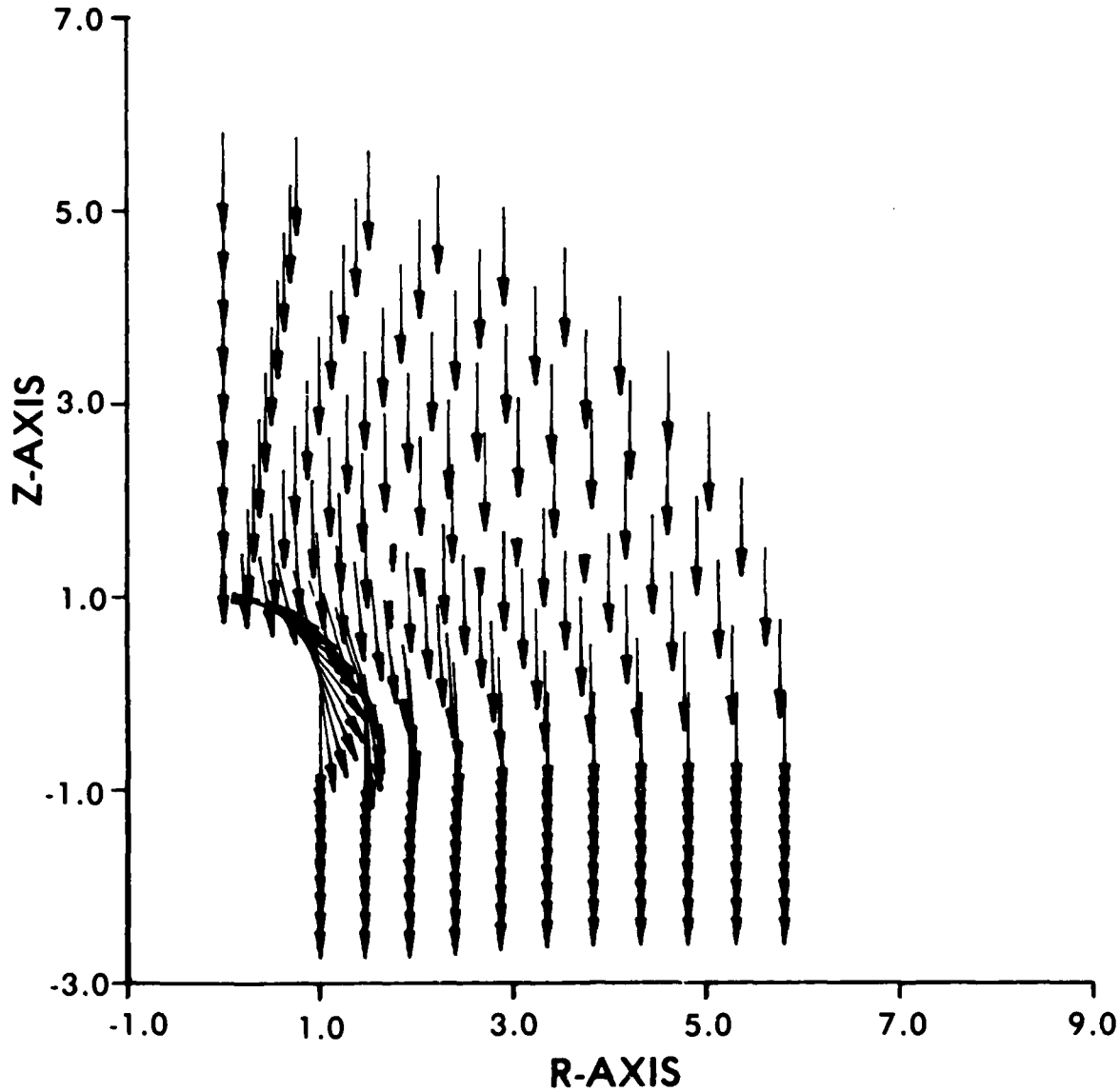

Figure 3: Velocity Field in the Target Material (α = 4.0).

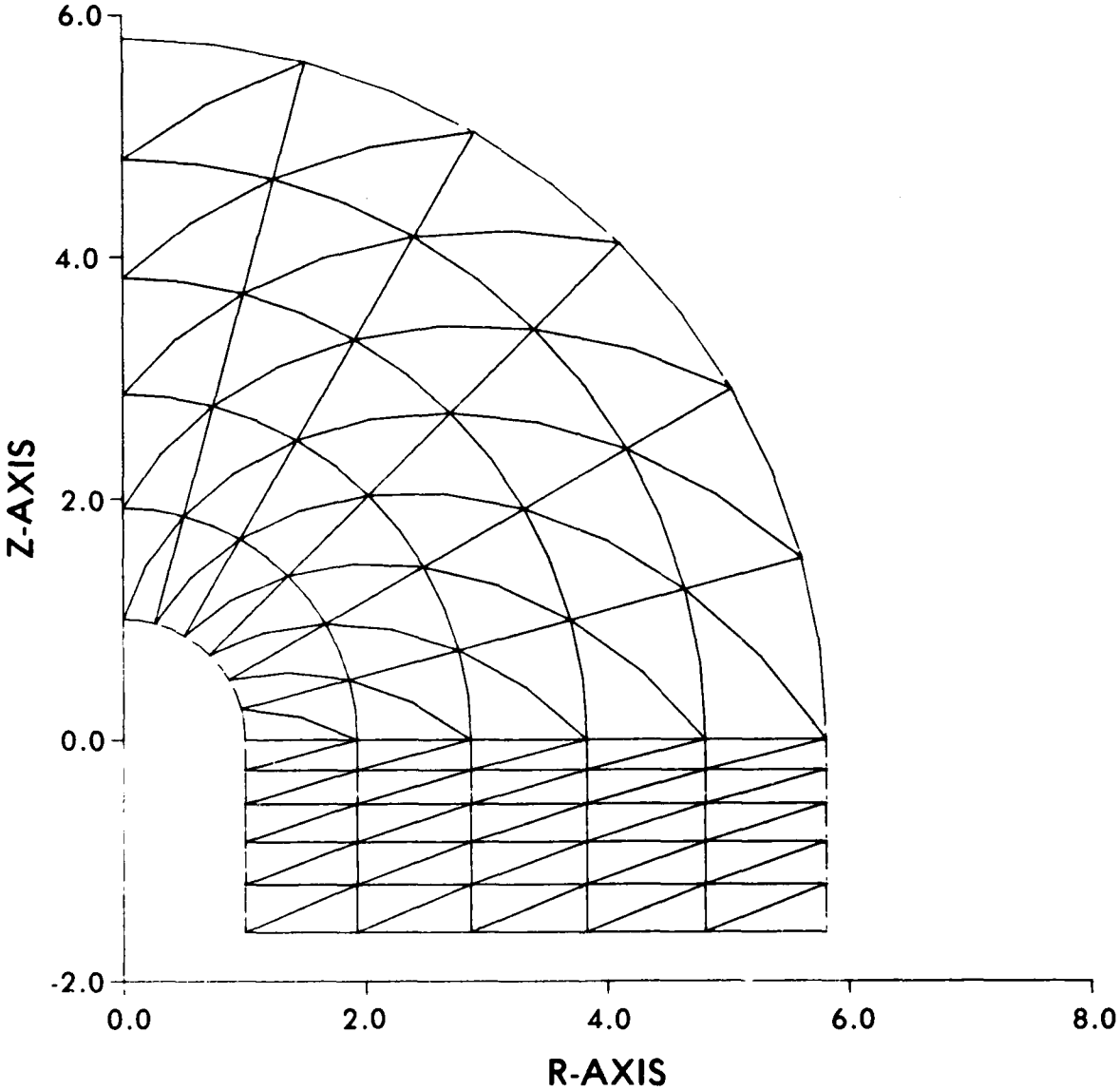

Figure 2: Finite Element Grid Used.

where m is the iteration number. For $\alpha < 2$, the initial solution was taken to be zero everywhere, and for $\alpha \geq 2$, the solution for a smaller value of α was taken as the initial solution. The iterative process was stopped when, at each nodal point,

$$||\underset{\sim}{v}^m - \underset{\sim}{v}^{m-1}|| \leq 0.01\ ||\underset{\sim}{v}^{m-1}||, \tag{10}$$

where the norm is defined by $||\underset{\sim}{v}|| = (v_r^2 + v_z^2)^{1/2}$.

IV. COMPUTATION AND DISCUSSION OF RESULTS

A computer code employing 6-noded isoparametric triangular elements has been written to solve the problem described above. Both the trial solution $(\underset{\sim}{v},p)$ and the test functions $(\underset{\sim}{\phi},\psi)$ are taken to belong to the same space of functions. Whereas, for the triangular element, $\underset{\sim}{v}$ is defined in terms of its values at all 6 nodal points, the pressure field p is defined only in terms of its values at the corner nodes. The integrations in equations (6) are performed by using the 4-point Gaussian quadrature rule. Since the curved surface of the penetrator nose is not a natural coordinate surface for the cylindrical geometry, it was found to be easiest to enforce the boundary conditions there by using a Lagrange multiplier technique.

The accuracy of the developed code has been established by solving a hypothetical flow problem for an incompressible Navier-Stokes fluid with uniform viscosity. A body force field was calculated so as to satisfy the balance of linear momentum exactly for an assumed, analytically known velocity field, where the assumed velocities had the essential features of those expected in the penetrator problem. Then the code was used to compute the velocity and pressure fields for that body force. The computed fields agreed very well with those known analytically. An important difference between the test problem and the penetration problem is that in the former the shear viscosity is taken to be constant, whereas in the latter, it depends on the rate of deformation. Since only a simple modification in the computer code is needed to incorporate this feature, it seems reasonable to assume that the computed solution is close to an analytical solution of the problem.

Figure 3 shows the velocity field in the target material for $\alpha = 4.0$. The velocity fields for other values of α have a similar pattern. Target points that lie to the rear of the center of the penetrator nose move parallel to the axis of the penetrator. Target points that lie ahead of the penetrator nose and within one penetrator diameter from it have a noticeable radial component of velocity. The distribution of normal traction on the penetrator nose for various values of α is plotted in Figure 4. (See Table 1 for identification of the various lines in this and subsequent figures.) Whereas the stress increases with α at the nose tip, it decreases at the sides of the nose. The value of the normal stress for $\theta = 45^\circ$ seems to be independent of α, at least for the range of values of α studied. For $\alpha = 6.15$ the normal stress at approximately $\theta = 83^\circ$ becomes negative, indicating a tendency for the target material to separate from the penetrator nose. Since our formulation of the problem does not allow for separation to occur, we seem to have reached the upper limit for the validity of the calculation, at least for the hemispherical nose shape.

Each term is evaluated on $r = 0$, s_{zz} is the deviatoric component of stress, and z is measured from the tip of the nose. Figure 13 shows the contributions from the various components in this formula as computed for $\alpha = 5.43$. Since the target material becomes nearly rigid a short distance away from the penetrator nose, the computation of the integrand in (12), which requires differences and divisions with small numbers, is unreliable for $z > 0.6$ or so, so that after that point, the upper bounding line was simply extended horizontally. Note that the integral term in (12) contributes substantially to the total and that the deviatoric component seems to stay constant at approximately 0.75 out of a total of 8.5.

Since the target deformation is essentially zero at some distance inside the boundary EFA, and since deformations are essentially independent of z near the boundary AB, it seems reasonable to assume that the target region chosen for computations is sufficient to obtain a good description of the deformation in the vicinity of the penetrator nose.

V. CONCLUSIONS

For the range of values of α studied, noticeable deformation of the target material occurs only at points that are less than three penetrator radii away from the penetrator, and the target seems to deform farther to the side than ahead of the penetrator. The target material adjacent to the sides of the penetrator appears to extrude rearwards in a uniform block that is separated from the bulk of the stationary target by a narrow region with a sharp velocity gradient, but the highest strain rates occur just ahead of the penetrator nose.

Maximum normal stresses occur at the nose tip, as might be expected, and fall off rapidly away from that point. At the higher values of α, flow separation seems to be indicated at the sides of the nose. The retarding force was found to be a weak linear function of α, and gradients of shear stress were found to make a strong contribution to the momentum integral along the axial streamline.

The kinematics and stress fields found in this paper should prove useful in devising or checking the results from simpler engineering theories of penetration.

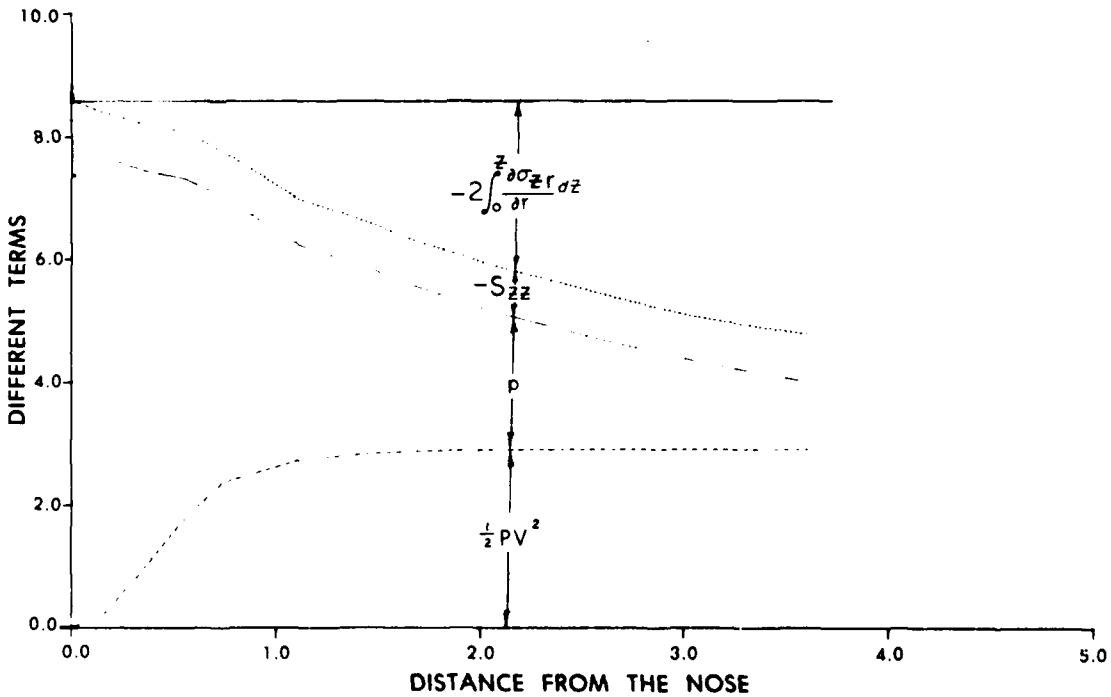

Figure 13: Contributions to the Integral Formula (12).

REFERENCES

1. Tate, A., "A Theory for the Deceleration of Long Rods After Impact," J. Mech. Phys. Sol. 15, 1967, 387-399.

2. Tate, A., "Further Results in the Theory of Long Rod Penetration," J. Mech. Phys. Sol. 17, 1969, 141-150.

3. Wright, T. W., "A Survey of Penetration Mechanics for Long Rods," in Lecture Notes in Engineering, Vol. 3, Computational Aspects of Penetration Mechanics, Eds., J. Chandra and J. Flaherty, Springer-Verlag, New York, 1983.

4. Ravid, M. and Bodner, S. R.,"Dynamic Perforation of Visco-plastic Plates by Rigid Projectiles," Int. J. Eng. Sci. 21, 1983, 577-591.

5. Prager, W. and Hodge, P., Theory of Perfectly Plastic Solids, Dover Publ., New York, 1968.

6. Becker, E., Carey, G., and Oden, J. T., Finite Elements, An Introduction, Vol. 1, Prentice-Hall, Englewood Cliffs, NY, 1981.

7. Pidsley, P. H., "A Numerical Study of Long Rod Impact Onto a Large Target," J. Mech. Phys. Sol. 32, 1984, 315-333.

DISTRIBUTION LIST

No. of Copies	Organization
12	Administrator Defense Technical Info Center ATTN: DTIC-DDA Cameron Station Alexandria, VA 22304-6145
2	Director Defense Advanced Research Projects Agency ATTN: Tech Info Dr. E. Van Reuth 1400 Wilson Boulevard Arlington, VA 22209
1	Deputy Assistant Secretary of the Army (R&D) Department of the Army Washington, DC 20310
1	HQDA DAMA-ART-M Washington, DC 20310
1	Commandant Command and General Staff College ATTN: Archives Fort Leavenworth, KS 66027
1	Commander US Army War College ATTN: Lib Carlisle Barracks, PA 17013
1	Commander US Army Materiel Command ATTN: AMCDRA-ST 5001 Eisenhower Avenue Alexandria, VA 22333-0001
7	Commander Armament R&D Center US Army AMCCOM ATTN: SMCAR-TSS SMCAR-TDC SMCAR-LC, J. Frasier SMCAR-LCA, T. Davidson SMCAR-SC, J. D. Corrie J. Beetle E. Bloore Dover, NJ 07801
1	Commander US Army Armament, Munitions and Chemical Command ATTN: SMCAR-ESP-L Rock Island, IL 61299
1	Director Benet Weapons Laboratory Armament R&D Center US Army AMCCOM ATTN: SMCAR-LCB-TL Watervliet, NY 12189
6	Commander Benet Weapons Laboratory ATTN: Dr. M. A. Hussain Dr. Julian Wu Dr. John Underwood Mr. D. P. Kindall Dr. J. Throup Dr. E. Schneider Watervliet, NY 12189
1	Commander US Army Aviation Research and Development Command ATTN: AMSAV-E 4300 Goodfellow Boulevard St. Louis, MO 63120

PREVIOUS PAGE IS BLANK

DISTRIBUTION LIST

No. of Copies	Organization
1	Commander US Army Communications - Electronics Command ATTN: AMSEL-ED Fort Monmouth, NJ 07703
1	Commander US Army Electronics Research and Development command Technical Support Activity ATTN: DELSD-L Fort Monmouth, NJ 07703-5301
1	Commander US Army Harry Diamond Laboratory ATTN: DELHD-TA-L 2800 Powder Mill Road Adelphi, MD 20783
1	Commander US Army Development and Employment Agency ATTN: MODE-TED-SAB Fort Lewis, WA 98433
1	Commander US Army Missile Command ATTN: AMSMI-R Redstone Arsenal, AL 35898
1	Commander US Army Missile Command ATTN: AMSMI-YDL Redstone Arsenal, AL 35898
1	Commander US Army Belvoir R & D Center ATTN: STRBE-WC Tech Lib (Vault), Bldg 315 Ft. Belvoir, VA 22060-5606
1	Commander US Army Natick Research and Development Laboratory ATTN: DRXRE, Dr. D. Sieling Natick, MA 01762
1	Commander US Army Tank Automotive Command ATTN: AMSTA-TSL Warren, MI 48090
1	Director US Army TRADOC Systems Analysis Activity ATTN: ATAA-SL White Sands Missile Range, NM 88002
1	Commander US Army Electronics Research and Development Command ATTN: Tech Lib Fort Huachuca, AZ 85613
1	Commandant US Army Infantry School ATTN: ATSH-CD-CSO-OR Fort Benning, GA 31905
1	Director US Army Advanced BMD Technology Center P.O. Box 1500, West Station Huntsville, AL 35807
3	Commander US Army Materiel and Mechanics Research Center ATTN: AMXMR-T, J. Mescall AMXMR-T, R. Shea AMXMR-H, S. C. Chou Watertown, MA 02172

DISTRIBUTION LIST

No. of Copies	Organization
5	Commander US Army Research Office ATTN: Dr. R. Weigle Dr. E. Saibel Dr. G. Mayer Dr. F. Smeideshoff Dr. J. Chandra P. O. Box 12211 Research Triangle Park, NC 27709-2211
2	Commander US Army Research and Standardization Group (Europe) ATTN: Dr. B. Steverding Dr. F. Rothwarf Box 65 FPO NY 09510
1	Office of Naval Research Department of the Navy ATTN: Code 402 Washington, DC 20375
1	Commander US Naval Air Systems Command ATTN: AIR-604 Washington, DC 20361
1	AUL (3T-AUL-60-118) Maxwell AFB, AL 36112
3	Commander Naval Surface Weapons Center ATTN: Dr. W. H. Holt Dr. W. Mock Tech Lib Dahlgren, VA 22448
3	Commander Naval Surface Weapons Center ATTN: Dr. R. Crowe Code R32, Dr. S. Fishman Tech lib Silver Spring, MD 20910
1	Director US Army Air Mobility Research and Development Laboratory Ames Research Center Moffett Field, CA 94035
5	Commander US Naval Research Laboratory ATTN: C. Sanday R. J. Weimer Code 5270, F. MacDonald Code 2020, Tech Lib Code 7786, J. Baker Washington, DC 20375
7	Commander US Naval Research Laboratory Engineering Materials Division ATTN: E. A. Lange G. R. Yoder C. A. Griffis R. J. Goode R. W. Judy, Jr. A. M. Sullivan R. W. Crooker Washington, DC 20375
5	Air Force Armament Laboratory ATTN: AFATL/DLODL J. Foster John Collins Joe Smith Guy Spitale Eglin AFB, FL 32542-5000
1	RADC (EMTLD, Lib) Griffiss AFB, NY 13441
1	AFELM, The Rand Corporation ATTN: Library-D 1700 Main Street Santa Monica, CA 90406

DISTRIBUTION LIST

No. of Copies	Organization
2	Air Force Wright Aeronautical Laboratories Air Force Systems Command Materials Laboratory ATTN: Dr. Theodore Nicholas Dr. John P. Henderson Wright-Patterson AFB, OH 45433
1	Director Environmental Science Service Administration US Department of Commerce Boulder, CO 80302
1	Director Lawrence Livermore Laboratory ATTN: Dr. M. L. Wilkins P. O. Box 808 Livermore, CA 94550
6	Sandia Laboratories ATTN: Dr. L. Davison Dr. P. Chen Dr. L. Bertholf Dr. W. Herrmann Dr. J. Nunziato Dr. S. Passman Albuquerque, NM 87115
1	Aeronautical Research Assoc. of Princeton, Inc. ATTN: Ray Gogolewski 1800 Old Meadow Road, #114 McLean, VA 22102
1	Director Jet Propulsion Laboratory ATTN: Lib (TDS) 4800 Oak Grove Drive Pasadena, CA 91109
1	Aeronautical Research Associates of Princeton, Incorporated ATTN: Ray Gogolewski 1800 Old Meadow Rd., #114 McLean, VA 22102
1	Honeywell, Inc. Govt. and Aerospace Products Division ATTN: Dr. Gordon Johnson 600 Second Street, NE Hopkins, MN 55343
1	AFWL/SUL Kirtland AFB, NM 87117
2	Orlando Technology, Inc. ATTN: Dr. Daniel Matuska Dr. John J. Osborn P. O. Box 855 Shalimar, FL 32579
7	SRI International ATTN: Dr. George Abrahamson Dr. Donald R. Curran Dr. Donald A. Shockey Dr. Lynn Seaman Mr. D. Erlich Dr. A. Florence Dr. R. Caligiuri 333 Ravenswood Avenue Menlo Park, CA 94025
1	Systems Planning Corporation ATTN: Mr. T. Hafer 1500 Wilson Boulevard Arlington, VA 22209
1	Terra-Tek, Inc. ATTN: Dr. Arfon Jones 420 Wakara Way University Research Park Salt Lake City, UT 84108
6	Brown University Division of Engineering ATTN: Prof. R. Clifton Prof. H. Kolsky Prof. L. B. Freund Prof. A. Needleman Prof. R. Asaro Prof. R. James Providence, RI 02912

DISTRIBUTION LIST

No. of Copies	Organization
3	California Institute of Technology Division of Engineering and Applied Science ATTN: Dr. J. Mikowitz Dr. E. Sternberg Dr. J. Knowles Pasadena, CA 91102
3	Carnegie-Mellon University Department of Mathematics ATTN: Dr. D. Owen Dr. M. E. Gurtin Dr. B. D. Coleman Pittsburgh, PA 15213
2	Catholic University of America School of Engineering and Architecture ATTN: Prof. A. Durelli Prof. J. McCoy Washington, DC 20017
6	Cornell University Department of Theoretical and Applied Mechanics ATTN: Dr. Y. H. Pao Dr. G. S. S. Ludford Dr. A. Ruoff Dr. J. Jenkins Dr. R. Lance Dr. F. Moon Ithaca, NY 14853
1	Denver Research Institute University of Denver ATTN: Dr. R. Recht P. O. Box 10127 Denver, CO 80210
2	Forrestal Research Center Aeronautical Engineering Lab. Princeton University ATTN: Dr. S. Lam Dr. A. Eringen Princeton, NJ 08540
1	Harvard University Division of Engineering and Applied Physics ATTN: Prof. J. R. Rice Cambridge, MA 02138
2	Iowa State University Engineering Research Laboratory ATTN: Dr. G. Nariboli Dr. A. Sedov Ames, IA 50010
2	Lehigh University Center for the Application of Mathematics ATTN: Dr. E. Varley Dr. R. Rivlin Bethlehem, PA 18015
1	New York University Department of Mathematics ATTN: Dr. J. Keller University Heights New York, NY 10053
1	North Carolina State University Department of Civil Engineering ATTN: Prof. Y. Horie Raleigh, NC 27607
1	Pennsylvania State University Engineering Mechanical Dept. ATTN: Prof. N. Davids University Park, PA 16802
3	Rensselaer Polytechnic Institute ATTN: Prof. E. H. Lee Prof. E. Krempl Prof. J. Flaherty Troy, NY 12181

DISTRIBUTION LIST

No. of Copies	Organization
2	Rice University ATTN: Dr. R. Bowen Dr. C. C. Wang P. O. Box 1892 Houston, TX 77001
1	Southern Methodist University Solid Mechanics Division ATTN: Prof. H. Watson Dallas, TX 75222
1	Southwest Research Institute ATTN: Dr. Charles Anderson 6220 Culebra Road P. O. Box Drawer 28510 San Antonio, TX 78284
2	Southwest Research Institute Department of Mechanical Sciences ATTN: Dr. U. Kindholm Dr. W. Baker 8500 Culebra Road San Antonio, TX 78228
1	Temple University College of Engineering Technology ATTN: Dr. R. Haythornthwaite Dean Philadelphia, PA 19122
4	The Johns Hopkins University ATTN: Prof. R. B. Pond, Sr. Prof. R. Green Prof. W. Sharpe Prof. J. Bell 34th and Charles Streets Baltimore, MD 21218
1	Tulane University Dept of Mechanical Engineering ATTN: Dr. S. Cowin New Orleans, LA 70112
3	University of California ATTN: Dr. M. Carroll Dr. W. Goldsmith Dr. P. Naghdi Berkeley, CA 94704
1	University of California Dept of Aerospace and Mechanical Engineering Science ATTN: Dr. Y. C. Fung P. O. Box 109 La Jolla, CA 92037
1	University of California Department of Mechanics ATTN: Dr. R. Stern 504 Hilgard Avenue Los Angeles, CA 90024
1	University of California at Santa Barbara Dept of Mechanical Engineering ATTN: Prof. T. P. Mitchel Santa Barbara, CA 93106
1	University of Dayton Research Institute ATTN: Dr. S. J. Bless Dayton, OH 45469
1	University of Delaware Dept of Mechanical Engineering ATTN: Prof. J. Vinson Newark, DE 19711
1	University of Delaware Dept of Mechanical and Aerospace Engineering ATTN: Dr. Minoru Taya Newark, DE 19711

DISTRIBUTION LIST

No. of Copies	Organization
3	University of Florida Dept. of Engineering Science and Mechanics ATTN: Dr. C. A. Sciammarilla Dr. L. Malvern Dr. E. Walsh Gainesville, FL 32611
2	University of Houston Department of Mechanical Engineering ATTN: Dr. T. Wheeler Dr. R. Nachlinger Houston, TX 77004
1	University of Illinois ATTN: Dean D. Drucker Urbana, IL 61801
1	University of Illinois Dept. of Theoretical and Applied Mechanics ATTN: Dr. D. Carlson Urbana, IL 61801
1	University of Illinois at Chicago Circle College of Engineering Dept. of Materials Engineering ATTN: Dr. T. C. T. Ting P. O. Box 4348 Chicago, IL 60680
2	University of Kentucky Dept. of Engineering Mechanics ATTN: Dr. M. Beatty Prof. O. Dillon, Jr. Lexington, KY 40506
1	University of Maryland Department of Mathematics ATTN: Prof. S. Antman College Park, MD 20740
1	University of Minnesota Dept. of Aerospace Engineering and Mechanics ATTN: Prof. J. L. Erickson 107 Akerman Hall Minneapolis, MN 55455
1	University of Pennsylvania Towne School of Civil and Mechanical Engineering ATTN: Prof. Z. Hashin Philadelphia, PA 19104
4	University of Texas Department of Engineering Mechanics ATTN: Dr. M. Stern Dr. M. Bedford Prof. Ripperger Dr. J. T. Oden Austin, TX 78712
1	University of Washington Dept. of Aeronautics and Astronautics ATTN: Dr. Ian M. Fyfe 206 Guggenheim Hall Seattle, WA 98105
2	Washington State University Department of Physics ATTN: Dr. R. Fowles Dr. G. Duvall Pullman, WA 99163
2	Yale University ATTN: Dr. B.-T. Chu Dr. E. Onat 400 Temple Street New Haven, CT 06520
1	University of Missouri - Rolla Department of Engineering Mechanics ATTN: Romesh C. Batra Rolla, MO 65401-0249

DISTRIBUTION LIST

No. of Copies	Organization
	Aberdeen Proving Ground
	Dir, USAMSAA ATTN: AMXSY-MP, H. Cohen AMXSY-D
	Cdr, USATECOM ATTN: AMSTE-TO-F
	Cdr, CRDC, AMCCOM ATTN: SMCCR-RSP-A SMCCR-MU SMCCR-SPS-IL

USER EVALUATION SHEET/CHANGE OF ADDRESS

This Laboratory undertakes a continuing effort to improve the quality of the reports it publishes. Your comments/answers to the items/questions below will aid us in our efforts.

1. BRL Report Number_____ Date of Report_____

2. Date Report Received_____

3. Does this report satisfy a need? (Comment on purpose, related project, or other area of interest for which the report will be used.)_____

4. How specifically, is the report being used? (Information source, design data, procedure, source of ideas, etc.)_____

5. Has the information in this report led to any quantitative savings as far as man-hours or dollars saved, operating costs avoided or efficiencies achieved, etc? If so, please elaborate._____

6. General Comments. What do you think should be changed to improve future reports? (Indicate changes to organization, technical content, format, etc.)

CURRENT ADDRESS

Name

Organization

Address

City, State, Zip

7. If indicating a Change of Address or Address Correction, please provide the New or Correct Address in Block 6 above and the Old or Incorrect address below.

OLD ADDRESS

Name

Organization

Address

City, State, Zip

(Remove this sheet along the perforation, fold as indicated, staple or tape closed, and mail.)

FOLD HERE

tor
my Ballistic Research Laboratory
AMXBR-OD-ST
een Proving Ground, MD 21005-5066

NO POSTAGE
NECESSARY
IF MAILED
IN THE
UNITED STATES

FFICIAL BUSINESS
TY FOR PRIVATE USE. $300

BUSINESS REPLY MAIL
FIRST CLASS PERMIT NO 12062 WASHINGTON, DC
POSTAGE WILL BE PAID BY DEPARTMENT OF THE ARMY

Director
US Army Ballistic Research Laboratory
ATTN: AMXBR-OD-ST
Aberdeen Proving Ground, MD 21005-9989

FOLD HERE

END

FILMED

10-85

DTIC